ADVANCING EARTH AND SPACE SCIENCES

JGR Atmospheres

RESEARCH ARTICLE

10.1029/2023JD039247

Correspondence of Drought Occurrences at Multi-Temporal Scales Between North China and Upper Hanjiang River

Xiaodan Zhang[1,2], Guoyu Ren[1,3], Takehiko Mikami[2], Jun Matsumoto[2], and Guowei Yang[1,3]

[1]Department of Atmospheric Science, School of Environmental Studies, China University of Geosciences, Wuhan, China, [2]Faculty of Urban Environmental Sciences, Department of Geography, Tokyo Metropolitan University, Tokyo, Japan, [3]Laboratory for Climate Studies, National Climate Center, China Meteorological Administration, Beijing, China

Key Points:

- There is a relatively significant co-drought in North China and the Upper Hanjiang River at multi-time scales
- When extreme droughts occurred in North China, there was a 52% probability that the Upper Hanjiang River was dry
- Similar drought and flood variability cycles exist on different time scales in North China and the Upper Hanjiang River

Supporting Information:

Supporting Information may be found in the online version of this article.

Correspondence to:

G. Ren,
guoyoo@cma.cn

Citation:

Zhang, X., Ren, G., Mikami, T., Matsumoto, J., & Yang, G. (2023). Correspondence of drought occurrences at multi-temporal scales between North China and Upper Hanjiang River. *Journal of Geophysical Research: Atmospheres*, *128*, e2023JD039247. https://doi.org/10.1029/2023JD039247

Received 13 MAY 2023
Accepted 18 OCT 2023

Author Contributions:

Conceptualization: Guoyu Ren
Data curation: Xiaodan Zhang
Formal analysis: Xiaodan Zhang
Funding acquisition: Guoyu Ren
Investigation: Xiaodan Zhang
Methodology: Guoyu Ren, Takehiko Mikami, Jun Matsumoto
Project Administration: Guoyu Ren
Resources: Xiaodan Zhang, Guowei Yang
Software: Xiaodan Zhang, Guowei Yang
Supervision: Guoyu Ren, Takehiko Mikami, Jun Matsumoto
Validation: Xiaodan Zhang
Visualization: Xiaodan Zhang
Writing – original draft: Xiaodan Zhang
Writing – review & editing: Xiaodan Zhang

Abstract

Using the drought and flood grades, the historical co-drought probabilities of the water source area (i.e., the Upper Hanjiang River or UH) and the receiving area (i.e., North China or NC) of the Middle Route of the South-to-North Water Diversion project from 1470 to 2017 were analyzed. It was found that there is relatively high possibility for co-droughts to occur in the UH and NC at interannual to multi-decadal time scales. When extreme drought occurred in NC, there was a 52% probability that the UH was on the drier side and even a 40% probability of severe drought. During the three typical severe drought events that occurred mainly in NC (i.e., 1637–1643, 1877–1878, and 1997–2002), severe droughts also appeared in the UH, with 1877–1878 even more severe than in NC. Among the seven driest years of the study period in NC (i.e., 1640, 1641, 1832, 1920, 1965, 1968, and 1997), only 1832 was wet in the UH, and 1920 even experienced the same severe region-wide drought as NC did. Furthermore, when severe consecutive droughts occurred in NC, there was at least a 66% probability that the UH was also experiencing a drought. In addition, there were obvious cycles of drought and flood variability of around 3–6 years, 10 years, 30 years, and 55–80 years in both the UH and NC. These findings are of importance to in-depth understanding of the regional drought variability and its mechanism at varied temporal scales and the effective management of the world-class hydro project.

Plain Language Summary

The co-drought probabilities of the water source area (the Upper Hanjiang River) and receiving area (North China) of the Middle Route of the South-to-North Water Diversion project at different time scales from 1426 to 2017 were analyzed. It was found that there is relatively high possibility for co-droughts to occur in both areas at interannual to multi-decadal time scales. Particularly, when extreme droughts occurred in North China, there was a 52% probability that the Upper Hanjiang River was also dry and even a 40% probability of severe droughts. When severe consecutive droughts occurred in North China, there was at least a 66% probability that the Upper Hanjiang River was also experiencing a drought. In addition, there are similar drought and flood variability cycles on different time scales in North China and the Upper Hanjiang River.

1. Introduction

Water resources are basic natural resources and strategic economic resources; under the current climate change context, water scarcity has become a global problem that cannot be ignored (Cosgrove & Loucks, 2015; Hoekstra, 2014; Xia & Shi, 2016). The IPCC's Sixth Assessment Report (AR6) noted that global climate change has significantly altered global water cycle processes since the mid-20th century, with an overall increase in precipitation intensity, but unevenly distributed in terms of temporal and spatial variability, which caused the intensity and duration of droughts to increase in some regions, such as South Europe, West Africa, and Central Asia (Pörtner et al., 2022). As global warming intensifies, the potential for compound extreme heat-drought events will probably increase in many regions (Pörtner et al., 2022). China is one of the most affected countries by climate change and variability; since the early 20th century, China's climate has experienced a remarkable change, with the surface air temperature increasing at a rate of about 0.10°C/decade (Ren et al., 2012; Wen et al., 2019). Precipitation in China does not show a significant long-term trend, but in the last half-century, the occurrence of droughts is expanded in scope, especially increased in frequency and intensity in North China (NC) and Southwest China, exacerbating the conflict of water scarcity (Chen & Sun, 2015; Zhang et al., 2018a, 2020).

The regional distribution of water resources in China is uneven, with a general trend of decreasing from the southeast coast to the northwest inland, showing a basic state of more water in the South and less water in the

North, in which the NC (mainly the North China Plain) owns the least amount of water resources per capita and the highest rate of water use consumption, and is the most water-scarce region in China (Cheng et al., 2019; China South-to-North Water Diversion Project Codification Committee or SNWDCC 2018b; Ren, 2007). The NC includes Beijing, the capital of China, Tianjin, one of China's three major industrial bases, and the famous industrial cities such as Shijiazhuang, Baoding, and Tangshan, as well as being the base of China's grain, cotton and oil production and a major wheat producing area (SNWDCC, 2018b). However, with population growth, rapid economic development, the improvement of people's living standards, and the increased frequency and intensity of meteorological droughts induced by the decreased annual precipitation in the last two decades of the 20th century, the water scarcity in the NC is becoming more and more serious (Li et al., 2018; Ren, 2007; SNWDCC, 2018b; Zhang et al., 2013, 2020).

The South-to-North Water Diversion Project was initiated in 2002. It is the world's largest water diversion project, with three water diversion zones planned from the upper, middle, and lower reaches of the Yangtze River, respectively, forming three water diversion routes—the Western, Middle and Eastern Lines—and is one of the key engineering measures to alleviate the severe water shortage in NC (SNWDCC, 2018b). The first phase of the Middle Route of the South-to-North Water Diversion (MSNWD) project has a total length of 1,432.49 km, with 1,277.21 km of the main trunk canal and 155.28 km of the Tianjin trunk canal, providing water for domestic and industrial use to 19 large and medium-sized cities and more than 100 counties (cities) in the NC (including Beijing, Tianjin, Hebei and Henan Provinces) from the Danjiangkou Reservoir in the Upper Hanjiang River (UH; SNWDCC, 2018a). After 11 years of construction, the MSNWD project was officially opened on 12 December 2014, and the overall water consumption in the Hanjiang River basin (HRB) was expected to exceed 29 billion m^3 (Zhen et al., 2019); by 22 July 2022, the project had transferred more than 50 billion cubic meters of water and benefited more than 85 million people (China Government Web, 2022).

However, climate change and variability have led to an increase in the frequency and intensity of droughts and a decrease in the runoff in the MSNWD project area, which may have a negative impact on the water diversion (Qin et al., 2021). Previous studies analyzed the probability of co-drought in NC and the UH from the perspective of precipitation and runoff (e.g., Ban et al., 2018; Chen & Xie, 2012; Liu et al., 2018; Ren et al., 2011; Yu et al., 2018). These analyses generally found a positive correlation between the UH and NC, and a higher possibility for the two areas to concurrently experience a meteorological drought based on observational data. However, due to limitations of instrumental data length, most of these studies were focused on the modern period, and there is still great uncertainty in the correlation between precipitation/droughts of NC and the UH at inter-decadal, multi-decadal and centennial scales. Ren et al. (2011) used historical drought and flood grade (DFG) data in their analysis, but the proxy data was directly based on the previously published "Yearly Charts of Dryness/Wetness in China over the last 500 years" (China Meteorological Administration, 1982), and the study scopes had not been focused specifically on the UH water source area and NC water-receiving area.

In order to better understand and predict change and variability in precipitation and drought, it is necessary to first reveal the temporal and spatial patterns of precipitation/drought change and variability over historical periods applying updated data other than instrumental records (Ge et al., 2005; Hao et al., 2016; Yang & Han, 2014; Yang et al., 2009; Zheng et al., 2006, 2018). Therefore, we used updated DFGs (Zhang et al., 2022, 2023) to analyze the characteristics of drought changes in NC and the UH from 1470 to 2017, with a hope to provide scientific reference basis for further understanding decadal to centennial scale variability of precipitation/drought of the study areas and future water resources scheduling and decision making in the MSNWD project.

2. Study Area, Data and Methods

2.1. Study Area

The UH was selected from the same range as our previous study (Zhang et al., 2022; Figure 1). The Hanjiang River is the first largest tributary of the Yangtze River, originating in Ningqiang County, Hanzhong City, Shaanxi Province, and mainly flowing through Shaanxi, Henan, and Hubei Provinces before joining the Yangtze River in Wuhan City, Hubei Province. The UH is located between the Qinling Mountains and Dabashan Mountains, with narrow, deep, fast flowing rivers and abundant hydraulic resources. It belongs to the humid monsoon climate zone on the edge of the northern subtropics, with an overall mild climate and abundant rainfall, the average annual precipitation is 863.93 mm (1960–2010) (Yin, 2015). However, the seasonal distribution of precipitation

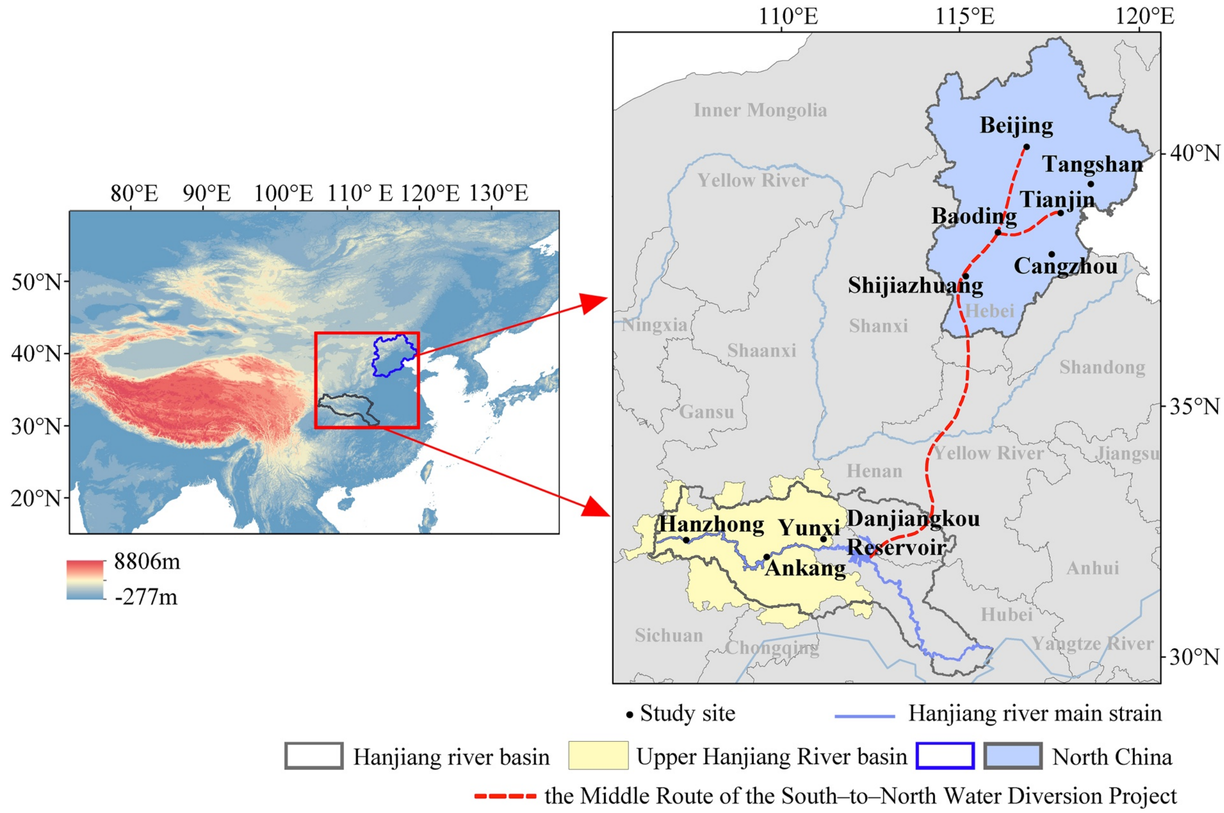

Figure 1. Study area and study sites distribution.

is uneven, with June to September accounting for about 60% of the annual precipitation and May to October accounting for about 75% of the annual runoff, making it the largest tributary of the Yangtze River in terms of runoff variation (1960–2010) (Yin, 2015).

NC is located at the margin of the East Asian summer monsoon with a subhumid warm temperate climate; rainfall in summer and autumn account for approximately 80% of the annual precipitation in this region (SNWDCC, 2018b). It has long been a socio-economically developed region in China due to its privileged location, flat terrain, abundant light and heat resources, rich land and mineral resources, as well as favorable water resources in historical periods (SNWDCC, 2018b). However, after the 1960s, NC began to suffer from water scarcity, and most of the rivers became seasonal, serving only the function of flood discharge during the flood season; by the late 1980s, most rivers were even more perennially unnavigable (SNWDCC, 2018b). Meanwhile, problems such as groundwater overdraft and water pollution are also very serious, and water scarcity has become a severe constraint on the socio-economic development of NC (Pörtner et al., 2022; SNWDCC, 2018b). In our study, the scope of NC is Beijing, Tangshan, Tianjin, Baoding, Cangzhou and Shijiazhuang (Figure 1).

2.2. Data and Methods

2.2.1. Data Sources and Reconstruction Methods

This study used historical drought and flood records and precipitation data from the instrumental period, and reconstructed the DFGs at three sites (Hanzhong, Ankang, and Yunxi sites; Figure 1) in the UH from 1470 to 2017, using five-grade classification based on The Atlas of Drought and Flood Distribution in China in the Last 500 Years (this atlas contains yearly distribution of DFG at 120 sites in China from 1470 to 1979; hereafter referred to as Atlas; Central Meteorological Bureau or CMB, 1981, now the China Meteorological Administration or CMA). The five-grade classification classifies drought and flood conditions according to their severity into Grade 1 flood, Grade 2 mild flood, Grade 3 normal, Grade 4 mild drought, and Grade 5 drought. Meanwhile, taking into account the frequency of occurrence of each grade, the ideal frequency criteria of 10%

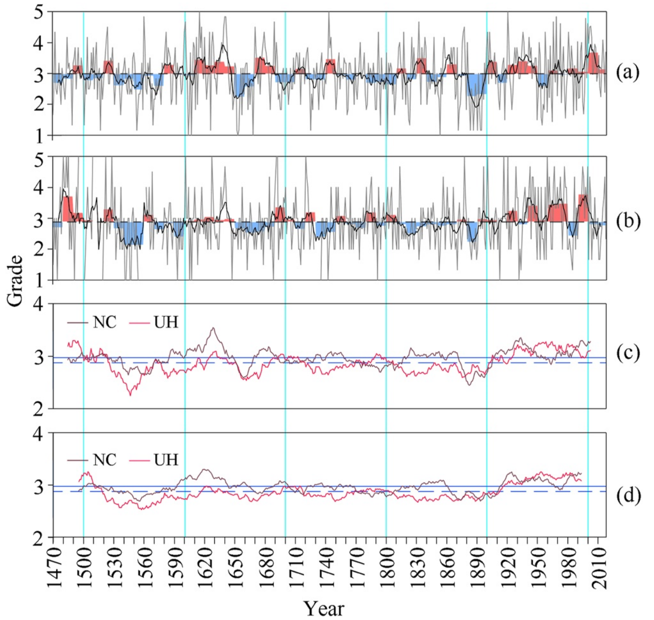

Figure 2. 1470–2017 DFG series in NC (a) and the UH (b), as well as 30-year (c) and 50-year (d) sliding average series for NC and the UH. For (a) and (b), the thin gray line indicates the yearly droughts and floods series; the bold black line indicates the 11-year sliding average droughts and floods series; black dashed line indicates average of DFG; the bar indicates the average DFG per decade, with orange representing above-average values and blue representing below-average values. For (c) and (d), the blue straight line indicates the DFG average for NC, and the blue dashed line indicates the DFG average for the UH. The blue vertical line separates the different centuries, with the first one on left indicating 1500, and the last one on right indicating 2000.

(Grade 1 flood and Grade 5 drought), 20%–30% (Grade 2 mild flood and Grade 4 mild drought), and 30%–40% (Grade 3 normal) were used for classification (CMB, 1981). Compared to the previous reconstruction of DFGs at Hanzhong and Ankang sites from 1470 to 2000 (CMB, 1981), we used more abundant historical sources in the reconstruction of each site on the UH, and used precipitation data from different sources (1951–2017; Yang & Li, 2014) to extend the time scale of DFGs for the instrumental period. Moreover, we added the Yunxi site to provide a clearer spatial resolution of historical drought and flood variability in the UH. The data sources, reconstruction methods and limitations were described in detail in our previous study (Zhang et al., 2022, 2023).

The historical DFGs for the six sites (Beijing, Tangshan, Tianjin, Baoding, Cangzhou and Shijiazhuang sites; Figure 1) in NC from 1470 to 1950 is derived from the Atlas (CMB, 1981). To analyze the variations of droughts and floods in NC after the beginning of the 21st century, as well as to ensure the consistency of the data sources, we used precipitation data from China National Surface Meteorological Station Homogenized Precipitation Data Set (V1.0) (Yang & Li, 2014), and reconstructed the DFGs for the instrumental period 1951–2017 in each site of NC with the five-grade classification method (CMB, 1981).

2.2.2. Arithmetic Average Method

The arithmetic average method is one of the simplest and most commonly used methods in statistics (Wei, 2007). We used this method to sum the DFGs for each site in NC and the UH and then averaged them to visualize the temporal characteristics of the overall drought and flood conditions. We also used the sliding average method, which is equivalent to a low-pass filter, to remove the influence of short-term or long-term fluctuations on the characteristics of droughts and floods to a certain extent (Wei, 2007), thus providing a more intuitive view of the inter-decadal and multi-decadal scales of droughts and floods in NC and the UH.

2.2.3. Wavelet Analysis and Ensemble Empirical Mode Decomposition (EEMD)

In this study, we used wavelet analysis and EEMD to analyze the drought and flood cycles in NC and the UH; both were implemented using Python, but the code was non-public. Wavelet analysis has good local discrimination in both the time and frequency domains, allowing the cycles of climate change to be analyzed on different time scales and the local characteristics of the cycle changes in the time series to be determined, thus providing a clear picture of the details of each cycle over time (Lau & Weng, 1995). The EEMD is an improved algorithm for empirical mode decomposition (EMD) (Wu & Huang, 2009) which effectively avoids the scale mixing problem of EMD by introducing white noise in the decomposition process and performing ensemble averaging, thus keeping the final decomposed eigenmode function physically unique (Huang et al., 1998). EEMD has strong local characteristics and the ability to extract non-significant weaker signals, allowing the time series to be decomposed into several physically meaningful intrinsic mode function (IMF), which is more suitable for analyzing non-smooth, non-linearly varying time series (Wu & Huang, 2009). The combination of wavelet analysis and EEMD results enables a more comprehensive capture of the variability of drought and flood cycles in NC and the UH.

3. Results

3.1. Correlation of Droughts and Floods Between NC and the UH

Based on the 1470–2017 yearly drought and flood series, the 11-year sliding average series, the average of DFGs per decade, and the 30 and 50 years sliding average series for NC and the UH (Figure 2; the averages of DFG in NC and the UH are 2.97 and 2.88, respectively), we found that, overall, when NC was relatively drought-prone,

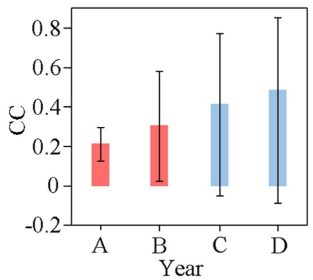

Figure 3. The correlation coefficients (CC) of DFG series between NC and the UH on a year-by-year basis (a), 10 years (b), 30 years (c), and 50 years (d). The error bars on the bar charts refer to the 90% confidence interval, and the red bars indicate that the test of significance was passed.

the UH also tended to be relatively drought-prone. It can be seen that during the drier periods in NC, 1490–1499, 1520–1529, 1610–1649, 1900–1909, 1920–1949, and 1960–1999, the UH was also relatively dry, especially during the two most prolonged periods of sustained drought in NC, that is, 1610–1649 and 1920–1949, the UH was also drought-prone. Furthermore, it is noteworthy that since the late 19th century, the frequency of co-droughts in the UH and NC was higher than before, and it seems to become a century-scale phenomenon.

To further verify the correlation between historical droughts and floods in NC and the UH at varied time scales, we calculated the correlation coefficients on year-by-year, 10-year, 30-year, and 50-year scales for NC and the UH, respectively. The calculation was made considering missing values for the UH (it has missing values in 1496–1500, 1510–1518, 1555–1561, 1574–1577, and 1729–1734) and possible autocorrelation in the time series (Bretherton et al., 1999; Santer et al., 2000). It was found that NC and the UH passed the 90% significance test on the year-by-year and 10-year scales (in which the year-by-year correlation passed the 95% significance test), but the correlations between the 30-year and 50-year scales were not significant on the statistical level, though they were higher than those on shorter time scales (Figure 3; See Supporting Information S1, Table S1).

According to the 30-year sliding correlation coefficient (Figure 4), it can be seen that during the period 1470–2017, the correlation between droughts and floods in NC and the UH is unstable. However, the correlations for the early 16th century, the second half of the 16th century to the mid-17th century, the late 17th century to the early 18th century, and the mid-19th century to the first half of the 20th century all passed the 90% significance test, indicating a relatively high correlation between drought and flood variations in NC and the UH during these periods. In particular, the second half of the 16th century to the mid-17th century were the periods of the strongest correlation between droughts and floods in NC and the UH throughout the study period, and the longest period of positive correlation lasted from the mid-19th century to the first half of the 20th century.

3.2. Probability of Concurrent Severe Droughts in NC and the UH

We calculated the annual occurrence frequency of Grade 5 drought (i.e., severe drought, described in detail in Zhang et al., 2022) at each site in NC and the UH from 1470 to 2017, as well as the number of years per 50 years of Grade 5 drought in NC and the UH, 1500–1999. From Figure 5 and Table S2 in Supporting Information S1, we can see that, overall, in the first half of the 17th century and from the mid-19th century to the present (−2017), the frequency of the Grade 5 drought in NC was the highest, while in these two periods, the frequency of the Grade 5 drought in the UH was also relatively high, especially after the mid-19th century, the frequency of Grade 5 drought in the UH was the highest in the whole study period, even surpassing that in NC.

To further verify the probability of concurrent severe droughts in the NC and the UH, we counted the top 10% of extreme drought years in NC from 1470 to 2017, a total of 50 years (according to the IPCC recommendations, 10% probability of occurrence means extreme events; Solomon et al., 2007). During these 50 years (Figure 6 and Table S3 in Supporting Information S1), the UH experienced a total of 26 years of droughts above Grade 3 (excluding Grade 3), including a total of 20 years above Grade 4 (including Grade 4; in particular, both NC and the UH experienced severe and continuous drought years from 1639 to 1641). It means that when extreme drought occurred in NC, there was a 52% probability that the UH also be on the drier side, with a 40% probability of severe drought events (i.e., Grade 4 and above). Furthermore, as can be seen from Table S3 in Supporting Information S1, although the phenomenon that the UH being relatively drought-prone during severe droughts in NC existed in every century, this co-drought, however, declined significantly in the 19th century, with a 25% probability of occurrence, while it increased significantly in the 20th century, with a 77% probability of occurrence. Based on our previous study (Zhang et al., 2022), the 19th century saw

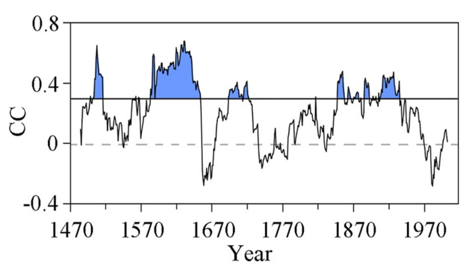

Figure 4. Correlation coefficient (CC) of 30-year sliding average DFG series between NC and the UH. The black straight line is the 90% significance threshold (the sample sizes were all assumed to be 30 years), and the blue portion indicates that the CC passed $p < 0.10$ significance test.

10.1029/2023JD039247

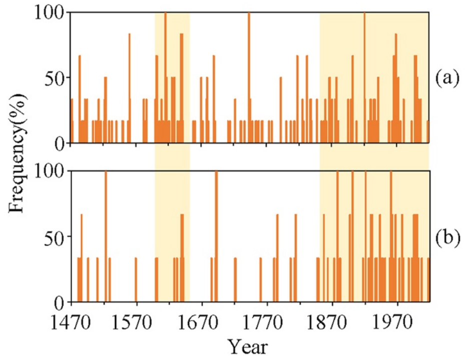

Figure 5. The yearly frequency of Grade 5 drought at each site in NC (a) and the UH (b), 1470–2017 (the number of sites with Grade 5 drought/total number of sites × 100%). The light yellow shading corresponds to 1600–1649 and 1850–2017, respectively.

fewer extreme droughts in the HRB, and in the 20th century, the frequency of extreme droughts increased significantly and was the highest in the last 592 years.

Based on the severity of drought disaster events that occurred in NC during the historical period and considering the completeness of the data from each site in the UH, we screened three typical drought disaster events from 1637 to 1643, 1877 to 1878, and 1997 to 2002 (Rong et al., 2008; Tan, 2003); meanwhile, we identified the seven years with the highest (i.e., driest) DFGs in NC from 1470 to 2017 and compared the DFGs in NC and the UH in the above years, as shown in Tables 1 and 2. It is clear that during the three typical severe drought events in NC (Table 1), the UH was similarly very dry, even more so in 1877–1878 than in NC, and the driest years in the UH and NC were the same, except for 1997–2002. In our previous study (Zhang et al., 2022), we selected other severe drought events in historical periods, including 1689–1692, 1928–1930, and 1942–1943, and found that the UH was also basically dry. From Table 2, during the seven driest years in NC (i.e., 1640, 1641, 1832, 1920, 1965, 1968, and 1997), only 1832 was wet in the UH, and 1968 was mildly dry, while the rest of the years had DFGs of 4 and above. In particular, there were even severe drought events (Grade 5) all over the region in the UH (Hanzhong, Ankang, and Yunxi sites) in 1920, as in NC.

Furthermore, we counted the consecutive drought years in NC from 1470 to 2017, when the average values of DFGs in each year were all Grade 4 or above, as well as the years when they were all above Grade 3.5, and calculated the average values of DFGs for these consecutive drought years. We then compared them with the average values of DFGs of the UH in the same period. As can be seen from Tables S4 and S5 in Supporting Information S1, during the study period, consecutive drought years with annual DFGs of Grade 4 or above were nine times in total in NC, and the UH experienced relative droughts on six occasions during the same period (1560–1561 had missing values), with the co-drought probability being at least 66.7%. Consecutive drought years with annual DFGs of above Grade 3.5 occurred with a total of 26 times in NC, and the UH experienced relative droughts on 18 occasions during the same period (1560–1561 had missing values), with the co-drought probability of at least 69.2%. That is, when relatively severe consecutive drought years occurred in NC, there was at least a 66% probability that the UH was also drought-prone at the same time.

3.3. Drought and Flood Cycles in NC and the UH

Comparative analyses of historical drought and flood cycles in NC and the UH are of great significance for the water transfer planning of the MSNWD project, the trend prediction of drought and flood, and the rational development and utilization of water resources (Wang et al., 2002). We conducted cycle analysis of droughts and floods in NC and the UH from 1578 to 2017 (because there are some missing data for the UH until 1578, and 1729–1734 gaps are filled in with the average values of the 30 years before and after) using EEMD (Figure 7, Table 3) and wavelet analysis (Figure 8), respectively. The EEMD decomposition resulted in seven IMFs with different time scales and fluctuation amplitudes from high to low frequencies (Table S6 in Supporting Information S1). For a more accurate and intuitive analysis of the cyclical variability characteristics on different time scales, we removed IMFs 6 and 7 with variance contributions below one, then combined IMFs 1 and 2 (both are interannual scale cycles; corresponding to the new IMF1 in Figure 7 and Table 3), 3 and 4 (both are interdecadal scale cycles; corresponding to the new IMF2 in Figure 7 and Table 3). And the new IMF3 (i.e., the combined IMF; multi-year intergenerational scale cycles) in Figure 7 and Table 3 corresponds to IMF5 after EEMD decomposition.

Figure 6. Distribution of extreme drought years in NC, 1470–2017. The red diamonds indicate DFGs above 4 (including Grade 4) in the UH in the same year as the extreme drought in NC; the yellow squares indicate DFGs above 3 (excluding Grade 3) in the UH in the same year as the extreme drought in NC; the small yellow dot indicates years when extreme drought occurred in NC without drought in the UH.

Combining the results of the above two methods, we found that the variability of drought and flood cycles in both NC and the UH was relatively

Table 1
Average of DFGs and the Driest Year in NC and the UH During the Typical Drought Events in NC

Extreme drought years		NC	UH
1637–1643	Average	4.21	3.67
	Driest year	1640, 1641	1640
1877–1878	Average	3.83	4.33
	Driest year	1877	1877
1997–2002	Average	4.21	3.61
	Driest year	1997	1999

smooth between the mid-18th and the early 19th centuries, and the following cycles of variation on interannual, interdecadal, and century scales can also be observed:

Interannual scale: Both NC and the UH have long-standing cycles of drought and flood variability of around 3–6 years. From Table 3, the IMF1 variance contribution reached 60.89% (NC) and 69.59% (UH), respectively, with its amplitude (Figure 7) and wavelet signals (Figure 8) showed basically a steady variation over most of the time period. However, there are some differences in the temporal distribution in the strength of the amplitude/signal of the 3–6 year cycle in these two regions. NC had a stronger amplitude/signal in the early 17th century and the second half of the 20th century, indicating a strong period of the 3–6 year cycle; a weaker amplitude/signal in the 18th century, indicating a weak period of the 3–6 year cycle. Overall, the amplitude/signal of the 3–6 year cycle in the UH was relatively weak until the mid-19th century but began to strengthen after the second half of the 19th century.

Interdecadal to multi-decadal scales: According to Table 3, there are interdecadal to multi-decadal cycles of drought and flood variability of around 12–30 years and 55 years in NC, with variance contributions of 18.1% and 3.54%, respectively; the UH has cycles of drought and flood variability of around 12–23 years and 55 years, with variance contributions of 13.32% and 2.88%, respectively. As a whole, the amplitude of the oscillations of both IMF2 and 3 (Figure 7) in NC is relatively stable, with IMF2 having the smallest amplitude from the mid-18th century to the early 19th century, indicating a weak 12–23 years cycle; from the second half of the 19th century to the present, IMF3 has a more intense amplitude than the earlier period, indicating a strong 55 years cycle during this time. In contrast, the UH IMF2 (Figure 7) has an overall stronger amplitude of oscillation, especially after the second half of the 19th century, as a period of strong drought and flood cycles of around 12–23 years. In contrast to NC, the signal of the 55 year cycle in the UH is not apparent (Figures 7 and 8), and only in the 17th century was the amplitude of the oscillation relatively pronounced.

The results of the wavelet analysis (Figure 8) showed that both NC and the UH have long-standing cycles of droughts and floods of around 10 and 30 years, but the strengths of the amplitude/signal have some differences in the temporal distributions. NC experienced weak cycle energies of around 30 years from the second half of the 18th century to the early 19th century, and significant cycle energies of around 30 years from the mid-17th century to the mid-18th century and from the mid-19th century to the present. In the UH the drought and flood cycles of around 30 years were stronger in energy after the mid-19th century, but shortened to around 20 years between the mid-19th and early 20th centuries, and then lengthened to around 30 years. In addition, there were significant drought and flood cycles of around 50 years in NC from the late 16th to the early 18th century. Though the same signal was not detected in the UH, but our previous studies indicated a multi-decadal cycle of around 50 years in the middle and lower HRB (Zhang et al., 2023).

Multi-decadal to century scales: From Figure 8, there is a significant multi-decadal to century-scale cycle of around 80 years in NC from the late 18th century to the present, and a cycle of around 70–80 in the UH from the late 16th to the mid-19th century. Although there are drought and flood cycles of around 70–80 years in both NC and the UH, there is a difference in timing, with those in NC more obvious in the last three centuries. However, from the mid-16th century to the present, the middle and lower HRB experienced long-term cycles with 80–100 years of drought and flood variability (Zhang et al., 2023).

In conclusion, it is clear that, on interannual and interdecadal scales, there are good similarities between the cycles of drought and flood variability in NC and the UH, and to some extent, this reflects the fact that some influential factors have common effects on the precipitation and droughts/floods in the two regions.

Table 2
DFGs in NC and the UH During the Driest Seven Years of NC, 1470–2017

Extreme drought years	NC	UH	Extreme drought years	NC	UH
1640	4.83	4.67	1965	4.67	4
1641	4.83	4	1968	4.83	3.33
1832	4.67	1.67	1997	4.78	4
1920	5	5			

4. Discussion

4.1. Implications for Water Supply of the MSNWD Project

Under the influence of climate change and variability, the intensity of drought in NC continues to increase, and, especially in the last 50 years, the frequency

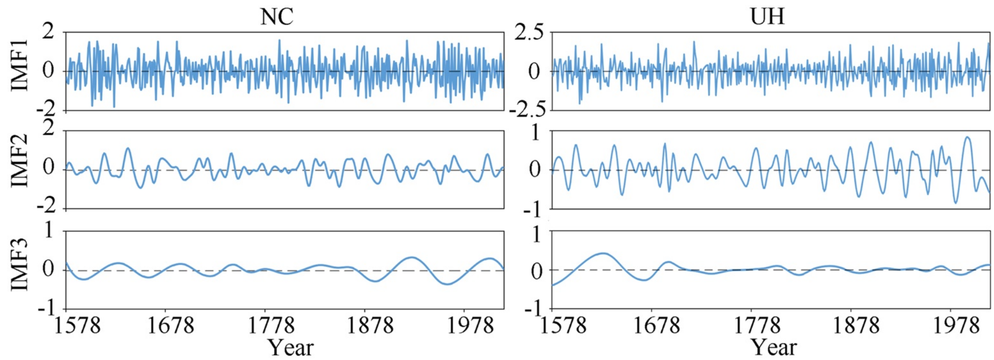

Figure 7. Results of EEMD decomposition of drought and flood series in NC and the UH from 1578 to 2017.

of extreme and persistent drought events in NC is increasing significantly (Ding et al., 2008; Qin et al., 2021; Ren et al., 2015; Zhang et al., 2018b); therefore, the MSNWD project is vital to the water supply of NC. However, previous studies showed that climate change has a negative impact on the water quantity in the UH (Ban et al., 2018); since the mid-20th century, the co-drought probability in the UH and the Haihe River basin (mainly flows through Beijing, Tianjin and Hebei Province) in NC were at historically high levels (Qin et al., 2021). Meteorological and hydrological data (1965–2016) indicated that while there was a weak increase in annual precipitation in the UH, the average annual temperature and annual potential evaporation also showed an upward trend; since 1990, the annual runoff depths in the UH and even in the whole HRB began to decline (Ban et al., 2018). Though the storage capacity of the Danjiangkou Reservoir increased after the early 21st century, the large inter-annual and seasonal variability in precipitation led to an uneven distribution of precipitation, causing dry spells or cut-offs to occur from time to time during the dry season (Qin et al., 2021). Based on an analysis of the dynamic changes in water storage in the Danjiangkou Reservoir from 2000 to 2016, Liu et al. (2018) found that the guaranteed rate of water supply from January to June was low, with May, in particular, being the most undersupplied, and the total guaranteed rate of the water supply from 2000 to 2016 only accounted for 17.6%.

According to previous studies (Ma et al., 2018; Ren et al., 2015; Zhai et al., 2017), though precipitation in NC increased after 2003, soil aridification is still continuing with significant and persistent drought events. Meanwhile, while precipitation in the UH will be on an upward trend in the future, the increase in evaporation makes the increase in runoff insignificant, runoff increase cannot effectively fill the water demand increase, and the water shortage in NC remains fundamentally unresolved (Qin et al., 2021). Yu et al. (2018) found that under RCP (Representative Concentration Pathway) 4.5 and RCP8.5 future climate change scenarios, the probability of co-drought in the UH and NC will rise in varying degrees compared to the present under both flood and non-flood season; especially during the flood season, the probability of experiencing the co-drought will significantly increase, while during the non-flood season, the probability of experiencing the co-severe drought will also significantly increase.

It is important to find out whether the co-drought in NC and the UH is simply due to the influence of climate change and variability in recent decades, or a long-standing phenomenon and regularity throughout history. Few previous researchers studied the probability of co-drought in the water source and receiving areas of the MSNWD project during the historical period, and for most of the long-series studies, the historical drought and

Table 3
Corresponding Drought and Flood Cycles for Each IMF (the Combined IMF), and the Variance Contribution (VC) and Correlation Coefficient (CC) to the Original Drought and Flood Series.

	NC			UH		
	IMF1	IMF2	IMF3	IMF1	IMF2	IMF3
Cycle	3.03–6.11	12.57–29.33	55	2.84–5.71	11.89–23.16	55
VC/%	60.89	18.1	3.54	69.59	13.32	2.88
CC	0.84**	0.52**	0.21**	0.89**	0.47**	0.13**

Note. **Represents passing the significance test of 0.01.

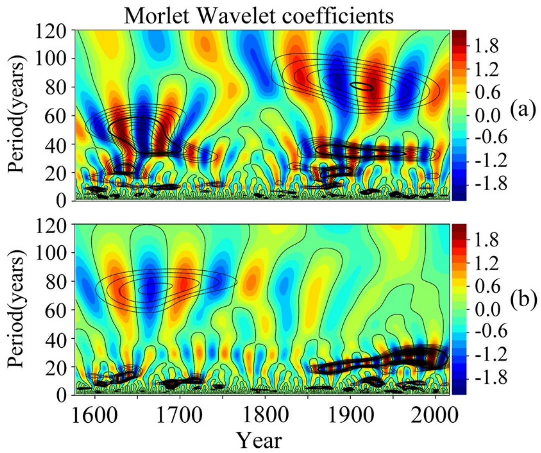

Figure 8. Results of wavelet analysis of drought and flood series in NC (a) and the UH (b), 1578–2017. Black contours indicate passing the 95% significance test of confidence, and larger color bar values indicate drier, and smaller values indicate wetter.

flood data were derived directly from Atlas (CMB, 1981). For example, Fang et al. (2018) found that the UH and the Haihe River basin were at relatively high risk of experiencing successive years of co-drought, based on DFGs from 1470 to 2000 in Atlas (CMB, 1981). In this study, we used the DFGs which we reconstructed previously with a longer time scale and higher spatial resolution of the UH (Zhang et al., 2022, 2023) to systematically analyze the drought and flood variability in NC and the UH from 1470 to 2017 at interannual, interdecadal and multi-decadal time scales. We found that although the frequency of droughts in the UH increased significantly since the 19th century leading to a higher frequency of co-drought with NC, there were significant co-droughts on interannual, and in less extent on multi-decadal, time scales in NC and the UH over nearly 600 years, and therefore the correspondence may not be just influenced by climate change and variability in recent decades.

Therefore, the concurrent droughts in NC and the UH are seeable not merely at interannual and interdecadal scales, as also shown in previous studies (Fang et al., 2018; Zhang et al., 2010), but at multi-decadal scales especially around 20–30 years. The occurrences of the co-droughts are not quite temporal scale-dependent. Possible causes of the co-droughts will be discussed below. However, this characteristic would be of importance for the operation and management of the MSNWD project. The co-droughts between NC and the UH at multi-decadal scales show that in both short and long time periods when precipitation is low and water shortage is serious in NC, the UH area will also suffer from droughts, and there is probably little water available in the water source area for being diverted to NC. The drought-drought encounters at an interannual scale may not cause big trouble, but the co-droughts may pose a serious challenge if they occur in a prolonged period of a decade or even two to three decades. Our analysis and findings show that the possibility for such a scenario to reappear cannot be ignored.

An interesting phenomenon is that the multi-decadal scale co-droughts seems to become more frequent in the 20th century. This may have been related to the more frequent occurrences of droughts after the 19th century, which had been shown in other regions including the middle and lower HRB (Zhang et al., 2022), the upper Yangtze river (Qin et al., 2020) and north Hubei province (Xu et al., 2010). Whether or not this phenomenon is caused by anthropogenic climate change needs to be further investigated. However, it indeed occurred under the background of global and regional warming. If the global warming continue in the future, as mentioned above and projected in many studies (Qin et al., 2021; Yu et al., 2018), the potential risk of the multi-decadal co-droughts in the MSNWD project deserves attention.

4.2. Possible Climatic Factors Influencing the Co-Drought in NC and the UH

The precipitation in most parts of China is influenced by the Asian monsoon (divided into two subsystems, the East Asian Monsoon and the Indian Monsoon), especially the East Asian summer monsoon (Ding et al., 2008). NC and the UH are located in the main rain bands of the East Asian summer monsoon; the advance and retreat of the East Asian summer monsoon are accompanied by the movement of the rain bands, which influences the changes in precipitation, droughts and floods in NC and the UH (Ding et al., 2020). It was found that during the period of the 1950s–1970s, when the East Asian summer monsoon was abnormally strong, China's rain bands moved northwards, and NC was relatively wet; after the late 1970s, the East Asian summer monsoon weakened significantly, the rain bands moved southwards, and NC was relatively dry (Gong & Ho, 2002; Zhai et al., 2005). In addition, previous studies found that there is a positive correlation between precipitation in NC and the Indian summer monsoon (e.g., Ding & Wang, 2005; Liu & Ding, 2008). Based on several sets of meteorological data and numerical simulation methods from 1951 to 2005, Liu and Ding (2008) explored in detail the intrinsic connection between the positive, negative, and positive tele-correlation patterns formed in North-West India through the Qinghai-Tibet Plateau to NC in terms of the dynamical and the thermal factor, and revealed the mechanism of the influence of the Indian summer monsoon on the precipitation in NC. They found that, when the Indian summer monsoon is strong, NC is more prone to precipitation; while in case of the weak Indian summer monsoon, NC is more prone to drought (Liu & Ding, 2008).

By the comparative analysis of the dates and circulation characteristics of the severe floods that occurred in the UH and the ravine region between Shanxi and Shannxi (located in the middle Yellow River), Yin (2015) found

10.1029/2023JD039247

that the East Asian summer monsoon and the Indian summer monsoon (i.e., the Asian monsoon) both influence precipitation in the UH. When the Asian monsoon is strong, the UH is more prone to heavy rainfall and floods; while the Asian monsoon is weak, the UH is more prone to droughts (Yin, 2015). Ding et al. (2008) analyzed the variation cycle of the East Asian summer monsoon in detail using 123 years (1880–2002) of precipitation data in China. They found that the East Asian summer monsoon has a distinct interannual variation cycle of 2–9 years and interdecadal to multi-decadal variation cycles of 10–14 years, 20–30 years, 40 years, and 60–80 years. According to the results of this study, there are long-term cycles of droughts and floods of around 3–6 years, 10 years, 30 years and 55–80 years in NC and the UH. Therefore, the co-drought between NC and the UH on interannual to multi-decadal scales is probably influenced by the strength of the monsoon.

In addition, our previous work (Zhang et al., 2023) found that historical drought and flood variability in the HRB during 1567–1990 showed relatively significant positive correlations with the Atlantic Multidecadal Oscillation (AMO) on the interdecadal to multi-decadal time scales. Although there is still lots of uncertainty about the impact of AMO on climate variability in East Asia (Li et al., 2009), Zhou et al. (2020) found that, during the Little Ice Age (1450–1850), when the AMO was in positive phases, precipitation tended to be low in eastern China (including Beijing, Tianjin and Hebei Province), especially in the Yangtze River basin. Furthermore, El Niño-Southern Oscillation (ENSO) has a significant 2–7 year interannual scale variation (Torrence & Webster, 1999), and sunspots have a significant 11 year variation (Friis-Christensen & Lassen, 1991), thus these factors may impact the drought variability of around 3–6 and 10 years, respectively in NC and the UH, as revealed in this analysis, and also the co-droughts in the two regions at interannual and interdecadal scales.

However, the climatic factors affecting precipitation or drought in eastern China are very complex, and the co-drought phenomenon in NC and the UH may also be influenced by the interaction of multiple climatic factors; moreover, the similarity of cycle lengths may not necessarily imply correlations, which requires further in-depth studies and analyses in our follow-up work.

4.3. Limitations

As proxy data, historical documents are characterized by "concerning only disasters but not normal conditions,"sometimes making drought/flood records incoherent and difficult to distinguish whether unrecorded years are "normal" or "omitted" (Zheng et al., 2014). Therefore, the reconstructed droughts in history in the UH may have certain uncertainty though with the droughts close to normal years in magnitude missed, but this uncertainty will not significantly affect the analysis results when a big sample has been used in the reconstruction. In addition, historical documents are generally focused on economically developed areas, with relatively few records from other surrounding areas, and also have a remarkable feature of "the closer to the present day, the more detailed and richer the record; the further from the present day, the less documented," which makes for an uneven spatial and temporal distribution of the historical records (Zheng et al., 2014). According to our previous study (Zhang et al., 2023), the historical records for the UH are relatively few compared to those for the middle and lower HRB, so some periods between 1470 and 1950 do not achieve very high confidence, but overall the results remain at high confidence level.

To summarize, it is important that the historical sources used to reconstruct the DFGs be carefully identified and validated. The primary historical sources for this study were strictly selected by previous researchers and were highly credible and reliable (Zhang et al., 2022, 2023). There is, of course, an unavoidable subjectivity in the reconstruction of climate series using historical documents, which cannot be avoided at all, even if we do not determine the grades simply on the basis of the descriptions of historical documents' statements and use other methodologies (Yang & Han, 2014). Therefore, the future reconstruction and analysis could be further improved if the uncertainties in the reconstruction of historical DFGs were to be further removed, with the help of applying more proxy data of varying accuracy, resolution and source, and cross-checking and analyzing in conjunction with other proxy data, for example, tree rings, ice cores, sediments, etc.

5. Conclusions

Using the DFGs series reconstructed from historical documents, we analyzed the probability of co-drought in NC and the UH from 1470 to 2017 on interannual, interdecadal and multi-decadal scales, respectively, and the results are as follows:

1. Correlation of the DFGs between NC and the UH passed the significance test on year-by-year ($p < 0.05$) and 10-year ($p < 0.10$) time scales. During the drier periods in NC, 1490–1499, 1520–1529, 1610–1649,

1900–1909, 1920–1949, and 1960–1999, the UH was also relatively dry, especially during the two most longest-lasting drought periods in NC, that is, 1610–1649 and 1920–1949, the UH was also relatively dry overall. The 30-year sliding correlation in NC and the UH is strongest from the second half of the 16th century to the mid-17th century, while the longest duration of positive correlation is from the mid-19th century to the first half of the 20th century.

2. NC experienced the highest frequency of Grade 5 droughts from the second half of the 16th century to the mid-17th century and from the mid-19th century to the present, while the UH in the same period also experienced a relatively high frequency of Grade 5 droughts, and especially since the middle of the 19th century, the frequency of Grade 5 droughts in the UH was the highest in the whole study period.
3. During the three typical major drought events in historical periods in NC, that is, 1637–1643, 1877–1878 and 1997–2002 megadroughts, the UH was also quite dry, with the 1877–1878 drought even more serious than that in NC. In the study period's seven driest years in NC, i.e., 1640, 1641, 1832, 1920, 1965, 1968, and 1997, only 1832 was relatively wet in the UH, and 1968 was mildly dry, while the rest of the years were at or above Grade 4.
4. When severe consecutive droughts occurred in NC, there was at least a 66% probability that the UH was also drought-prone at the same time, indicating a higher possibility for the simultaneous severe consecutive droughts to occur in history.
5. EEMD and wavelet analysis indicates that NC and the UH both have distinct cycles of drought and flood variability of around 3–6 years, 10 years, 30 years, and 55–80 years corresponding to the drought and flood variabilities at interannual, interdecadal, and multi-decadal time scales.

Data Availability Statement

Part of the data used in the present study is referred in the reference list. Other part of data is not publicly released due to the rules of data restriction.

Acknowledgments
This study was supported by the National Key R&D Program of China (2018YFA0605603) and China Scholarship Council under Grant 202106410037. We thank Editor Yongyun Hu for the help with this manuscript, and three anonymous reviewers for their constructive comments.

References

Ban, X., Zhu, B. Y., Shu, P., Du, H., & Lv, X. R. (2018). Trends and driving forces of meteorological and hydrological changes in the Hanjiang River Basin. *Resources and Environment in the Yangtze Basin*, *27*, 2817–2829. https://doi.org/10.11870/cjlyzyyhj201812018

Bretherton, C. S., Widmann, M., Dymnikov, V. P., Wallace, J. M., & Bladé, I. (1999). The effective number of spatial degrees of freedom of a time-varying field. *Journal of Climate*, *12*(7), 1990–2009. https://doi.org/10.1175/1520-0442(1999)012<1990:TENOSD>2.0.CO;2

Central Meteorological Bureau. (1981). The atlas of drought and flood distribution in China in the last 500 years [Dataset]. Book publisher.

Chen, F., & Xie, Z. H. (2012). Impact of climate change on precipitation abundance in the water source and receiving areas of the Middle Route of the South–to–North Water Diversion Project. *Climatic and Environmental Research*, *17*(2), 139–148. https://doi.org/10.3878/j.issn/j.issn.1006-9585.2011.10097

Chen, H. P., & Sun, J. Q. (2015). Drought response to air temperature change over China on the centennial scale. *Atmospheric and Oceanic Science Letters*, *8*(3), 113–119. https://doi.org/10.1080/16742834.2015.11447247

Cheng, X., Chen, L. D., Sun, R. H., & Jing, Y. C. (2019). Identification of regional water resource stress based on water quantity and quality: A case study in a rapid urbanization region of China. *Journal of Cleaner Production*, *209*, 216–223. https://doi.org/10.1016/j.jclepro.2018.10.175

China Government Web. (2022). Middle route of the south-to-north water diversion project has transferred more than 50 billion cubic meters of water and benefited more than 85 million people. Retrieved from http://www.gov.cn/xinwen/2022-07/26/content_5702827.htm

China Meteorological Administration. (1982). *Yearly charts of dryness/wetness in China over the last 500 years*. China Meteorological Press.

China South-to-North Water Diversion Project Codification Committee. (2018a). *China south-to-north diversion project (engineering & technology volume)*. China Meteorological Press.

China South-to-North Water Diversion Project Codification Committee. (2018b). *China south-to-north diversion project (pre-work volume)*. China Water&Power Press.

Cosgrove, W. J., & Loucks, D. P. (2015). Water management: Current and future challenges and research directions. *Water Resources Research*, *51*(6), 4823–4839. https://doi.org/10.1002/2014WR016869

Ding, Q. H., & Wang, B. (2005). Circumglobal teleconnection in the Northern Hemisphere summer. *Journal of Climate*, *18*(17), 3483–3505. https://doi.org/10.1175/JCLI3473.1

Ding, Y. H., Liu, Y. J., & Song, Y. F. (2020). The East Asian summer monsoon moisture conveyor belt and its impact on heavy rainfall and flooding in China. *Advances in Water Science*, *31*(05), 629–643. https://doi.org/10.14042/j.cnki.32.1309.2020.05.001

Ding, Y. H., Wang, Z. Y., & Sun, Y. (2008). Inter-decadal variation of the summer precipitation in East China and its association with decreasing Asian summer monsoon. Part I: Observed evidences. *International Journal of Climatology: A Journal of the Royal Meteorological Society*, *28*(9), 1139–1161. https://doi.org/10.1002/joc.1615

Fang, S. D., Liu, M., & Ren, Y. J. (2018). Water source and receiving areas of the middle route of the south–to–north water diversion project drought and flood characteristics and risk prediction. *Bulletin of Soil and Water Conservation*, *38*(06), 263–267+276. https://doi.org/10.13961/j.cnki.stbctb.2018.06.040

Friis-Christensen, E., & Lassen, K. (1991). Length of the solar cycle: An indicator of solar activity closely associated with climate. *Science*, *254*(5032), 698–700. https://doi.org/10.1126/science.254.5032.698

Ge, Q. S., Zheng, J. Y., Hao, Z. X., Zhang, P. Y., & Wang, W. C. (2005). Reconstruction of historical climate in China: High-resolution precipitation data from Qing Dynasty archives. *Bulletin of the American Meteorological Society*, *86*(5), 671–680. https://doi.org/10.1175/BAMS-86-5-671

Gong, D. Y., & Ho, C. H. (2002). Shift in the summer rainfall over the Yangtze River valley in the late 1970s. *Geophysical Research Letters*, *29*(10), 78-1–78-4. https://doi.org/10.1029/2001GL014523

Hao, Z. X., Zheng, J. Y., Zhang, X. Z., Liu, H. L., Li, M. Q., & Ge, Q. S. (2016). Spatial patterns of precipitation anomalies in eastern China during centennial cold and warm periods of the past 2000 years. *International Journal of Climatology*, *36*(1), 467–475. https://doi.org/10.1002/joc.4367

Hoekstra, A. Y. (2014). Water scarcity challenges to business. *Nature Climate Change*, *4*(5), 318–320. https://doi.org/10.1038/nclimate2214

Huang, N. E., Shen, Z., Long, S. R., Wu, M. L. C., Shih, H. H., Zheng, Q. A., et al. (1998). The empirical mode decomposition and the Hilbert spectrum for nonlinear and non-stationary time series analysis. *Proceedings of the Royal Society of London. Series A: Mathematical, Physical and Engineering Sciences*, *454*(1971), 903–995. https://doi.org/10.1098/rspa.1998.0193

Lau, W. K. M., & Weng, H. Y. (1995). Climate signal detection using wavelet transform: How to make a time series sing. *Bulletin of the American Meteorological Society*, *76*(12), 2391–2402. https://doi.org/10.1175/1520-0477(1995)076<2391:CSDUWT>2.0.CO;2

Li, R. N., Zheng, H., Huang, B. B., Xu, H. S., & Li, Y. K. (2018). Dynamic impacts of climate and land-use changes on surface runoff in the mountainous region of the Haihe River Basin, China. *Advances in Meteorology*, *2018*(2), 1–10. https://doi.org/10.1155/2018/3287343

Li, S. L., Wang, Y. M., & Gao, Y. Q. (2009). A review of the researches on the Atlantic multidecadal oscillation and its climate influence. *Transactions of Atmospheric Sciences*, *32*(3), 458–465. https://doi.org/10.3969/j.issn.1674-7097.2009.03.014

Liu, H., Yin, J., & Feng, L. (2018). The dynamic changes in the storage of the Danjiangkou Reservoir and the influence of the south-north water transfer project. *Scientific Reports*, *8*(1), 1–12. https://doi.org/10.1038/s41598-018-26788-5

Liu, Y. Y., & Ding, Y. H. (2008). Remote correlation analysis and numerical simulation of Indian summer monsoon and precipitation in North China. *Acta Meteorologica Sinica*, *66*(5), 789–799. https://doi.org/10.3321/j.issn:0577-6619.2008.05.012

Ma, Z. G., Fu, C. B., Yang, Q., Zheng, Z. Y., Lv, M. X., Li, M. X., et al. (2018). On the aridification of the North of China and its transitional changes. *Chinese Journal of Atmospheric Sciences*, *42*(04), 951–961. https://doi.org/10.3878/j.issn.1006-9895.1802.18110

Pörtner, H.-O., Roberts, D. C., Tignor, M., Poloczanska, E. S., Mintenbeck, K., & Alegría, A., et al. (2022). *Climate change 2022: Impacts, adaptation and vulnerability. Contribution of working Group II to the sixth assessment report of the intergovernmental panel on climate change*. Cambridge University Press.

Qin, D. H., Ding, Y. J., Zhai, P. M., Song, L. C., & Jiang, K. X. (2021). *Climate and ecological evolution in China: 2021*. Science Publishing House.

Qin, J., Shi, A. L., Ren, G. Y., Chen, Z. H., Yang, Y. D., Zhou, X. K., & Zhang, P. F. (2020). Severe historical droughts carved on rock in the Yangtze. *Bulletin of the American Meteorological Society*, *101*(6), 905–916. https://doi.org/10.1175/BAMS-D-19-0126.1

Ren, G. Y. (2007). *Climate change and water resources in China*. China Meteorological Press.

Ren, G. Y., Ding, Y. H., Zhao, Z. C., Zheng, J. Y., Wu, T. W., Tang, G. L., & Xu, Y. (2012). Recent progress in studies of climate change in China. *Advances in Atmospheric Sciences*, *29*(5), 958–977. https://doi.org/10.1007/s00376-012-1200-2

Ren, G. Y., Liu, H. B., Chu, Z. Y., Zhang, L., Li, X., Li, W., et al. (2011). Multi-time-scale climatic variations over eastern China and implications for the South–North Water diversion project. *Journal of Hydrometeorology*, *12*(4), 600–617. https://doi.org/10.1175/2011JHM1321.1

Ren, G. Y., Ren, Y. Y., Zhan, Y. J., Sun, X. B., Liu, Y. J., Chen, Y., & Wang, T. (2015). Temporal and spatial variation of precipitation in Mainland China II. Modern trends. *Advances in Science and Technology of Water Resources*, *26*(04), 451–465. https://doi.org/10.14042/j.cnki.32.1309.2015.04.001

Rong, Y. S., Duan, L. Y., & Xu, M. (2008). Climatic diagnostic analysis of continuing drought in North China, 1997-2002. *Arid Zone Research*, *25*(6). CNKI:SUN:GHQJ.0.2008-06-016.

Santer, B. D., Wigley, T. M. L., Boyle, J. S., Gaffen, D. J., Hnilo, J. J., Nychka, D., et al. (2000). Statistical significance of trends and trend differences in layer-average atmospheric temperature time series. *Journal of Geophysical Research*, *105*(D6), 7337–7356. https://doi.org/10.1029/1999JD901105

Solomon, S., Qin, D., Manning, M., Chen, Z., Marquis, M., Averyt, K. B., et al. (2007). *IPCC 2007: Climate change 2007: The physical science basis. Contribution of working Group I to the fourth assessment report of the intergovernmental panel on climate change*. Cambridge university press.

Tan, X. (2003). Research on the catastrophic drought in China in the past 500 years. *Journal of Disaster Prevention and Mitigation Engineering*, *2*, 77–83. CNKI:SUN:DZXK.0.2003-02-010.

Torrence, C., & Webster, P. J. (1999). Interdecadal changes in the ENSO–monsoon system. *Journal of Climate*, *12*(8), 2679–2690. https://doi.org/10.1175/1520-0442(1999)012<2679:ICITEM>2.0.CO;2

Wang, W. S., Ding, J., & Xiang, H. L. (2002). Research and prospects on the application of wavelet analysis in hydrology. *Advances in Water Science*, *13*(4), 515–520. https://doi.org/10.3321/j.issn:1001-6791.2002.04.021

Wei, F. Y. (2007). *Modern climate statistical diagnosis and prediction technology*. China Meteorological Press.

Wen, K. M., Ren, G. Y., Li, J., Zhang, A. Y., Ren, Y. Y., Sun, X. B., & Zhang, Y. Q. (2019). Recent surface air temperature change over mainland China based on an urbanization-bias adjusted dataset. *Journal of Climate*, *32*(10), 2691–2705. https://doi.org/10.1175/JCLI-D-18-0395.1

Wu, Z. H., & Huang, N. E. (2009). Ensemble empirical mode decomposition: A noise-assisted data analysis method. *Advances in Adaptive Data Analysis*, *1*(01), 1–41. https://doi.org/10.1142/S1793536909000047

Xia, J., & Shi, W. (2016). Research and perspectives on water security in China in a changing environment. *Journal of Hydraulic Engineering*, *47*(03), 292–301. https://doi.org/10.13243/j.cnki.slxb.20150937

Xu, X. C., Ge, Q. S., Zheng, J. Y., & Liu, C. W. (2010). Reconstruction of regional wet and dry series in Hubei Province for the last 500 years and its comparative analysis. *Geographical Research*, *29*(6), 1045–1055. https://doi.org/10.11821/yj2010060010

Yang, S., & Li, Q. X. (2014). Methodology for homogeneity analysis of precipitation series in China and improvement of dataset update [Dataset]. Climate Change Research, *10*(4), 276–281. https://doi.org/10.3969/j.issn.1673-1719.2014.04.008

Yang, Y. D., & Han, J. F. (2014). A study of screening methods for extreme climatic events in historical periods: An example of extreme drought sequences in the northwest millennium. *Historical Geography*, *30*, 10–29.

Yang, Y. D., Wang, M. S., & Man, Z. M. (2009). Methodological advances in historical climate research in China in the last three decades: Centered on documentary sources. *Collections of Essays On Chinese Historical Geography*, *24*(2), 5–13.

Yin, S. Y. (2015). *Research on extreme climate and hydrological events and their social impacts in the Upper Hanjiang River since historical periods*. Science Press.

Yu, J. Y., Xia, J., She, D. X., Zhou, L., & Li, T. S. (2018). Study on the drought encounter between the water source area of he middle route of the south–to–north water diversion project and the receiving area of the Haihe River. *South–to–North Water Transfers and Water Science & Technology*, *16*(01), 63–68+194. https://doi.org/10.13476/j.cnki.nsbdqk.20180010

Zhai, J. Q., Huang, J. L., Su, B. D., Cao, L. G., Wang, Y. J., Tong, J., & Fischer, T. (2017). Intensity–area–duration analysis of droughts in China 1960–2013. *Climate Dynamics*, *48*(1), 151–168. https://doi.org/10.1007/s00382-016-3066-y

Zhai, P. M., Zhang, X. B., Wan, H. H., & Pan, X. H. (2005). Trends in total precipitation and frequency of daily precipitation extremes over China. *Journal of Climate*, *18*(7), 1096–1108. https://doi.org/10.1175/JCLI-3318.1

Zhang, J. Y., He, R. M., Qi, J., Liu, C. S., Wang, G. Q., & Jin, J. L. (2013). Re-conceptualisation of water resources issues in North China. *Advances in Water Science*, *24*(03), 303–310. https://doi.org/10.14042/j.cnki.32.1309.2013.03.001

Zhang, J. Y., Wang, G. Q., Jin, J. L., He, R. M., & Liu, C. S. (2020). Evolution of river runoff and its changing characteristics in China, 1956-2018. *Advances in Water Science*, *31*(02), 153–161. https://doi.org/10.14042/j.cnki.32.1309.2020.02.001

Zhang, L. P., Qin, L. L., Zhang, D., & Zeng, S. D. (2010). A study of droughts and floods in the south-north water transfer central line water source area and the Haihe receiving area. *Resources and Environment in the Yangtze Basin*, *19*(8), 940–945.

Zhang, L. X., Wu, P. L., Zhou, T. J., & Chan, X. (2018b). ENSO transition from La Niña to El Niño drives prolonged spring–summer drought over North China. *Journal of Climate*, *31*(9), 3509–3523. https://doi.org/10.1175/JCLI-D-17-0440.1

Zhang, Q., Li, Q., Singh, V. P., Shi, P. J., Huang, Q. Z., & Peng, S. (2018a). Nonparametric integrated agrometeorological drought monitoring: Model development and application. *Journal of Geophysical Research: Atmospheres*, *123*(1), 73–88. https://doi.org/10.1002/2017jd027448

Zhang, X. D., Ren, G. Y., Bing, H., Mikami, T., Matsumoto, J., Zhang, P. F., & Yang, G. W. (2023). Reconstruction and characterization of droughts and floods in the Hanjiang River Basin, China, 1426–2017. *Climatic Change*, *176*(5), 1–21. https://doi.org/10.1007/s10584-023-03538-9

Zhang, X. D., Ren, G. Y., Yang, Y. D., Bing, H., Hao, Z. X., & Zhang, P. F. (2022). Extreme historical droughts and floods in the Hanjiang River Basin, China, since 1426. *Climate of the Past*, *18*(8), 1775–1796. https://doi.org/10.5194/cp-18-1775-2022

Zhen, W. Q., Wang, R., Guo, W., Kong, W. D., Wang, Z. W., & Zhao, A. X. (2019). Impacts of climate change on water transfer patterns in the Jianghan Plain. *Resources and Environment in the Yangtze Basin*, *28*(11), 2753–2762. https://doi.org/10.11870/cjlyzyyhj201911022

Zheng, J. Y., Ge, Q. S., Hao, Z. X., Liu, H. L., Man, Z. M., Hong, Y. J., & Fang, X. Q. (2014). Meteorological records in historical documents and methods for quantitative reconstruction of climate change. *Quaternary Sciences*, *34*(06), 1186–1196. https://doi.org/10.3969/j.issn.1001-7410.2014.06.07

Zheng, J. Y., Wang, W. C., Ge, Q. S., Man, Z. M., & Zhang, P. Y. (2006). Precipitation variability and extreme events in eastern China during the past 1500 years. *Terrestrial, Atmospheric and Oceanic Sciences*, *17*(3), 579. https://doi.org/10.3319/TAO.2006.17.3.579(A)

Zheng, J. Y., Yu, Y. Z., Zhang, X. Z., & Hao, Z. X. (2018). Variation of extreme drought and flood in North China revealed by document-based seasonal precipitation reconstruction for the past 300 years. *Climate of the Past*, *14*(8), 1135–1145. https://doi.org/10.5194/cp-14-1135-2018

Zhou, X., Lang, X., & Jiang, D. (2020). Teleconnections between the Atlantic multidecadal oscillation and eastern China summer precipitation during the medieval climate anomaly and little ice age. *The Holocene*, *30*(12), 1694–1705. https://doi.org/10.1177/0959683620950413